Clinical Cancer Investigation Journal-ISSN: 2278-0513

Cancer, a phenomenon in the interactive cycles between cosmic phenomena

Abstract

Cancer, a phenomenon that is controversial among scientists about how it is created, has shown structures that can be seen in other phenomena of the universe. Thus, we examine the structures and geometric regularity of the recorded images of two phenomena: MCF-7 Breast Cancer Cells and glioblastoma tumors. Although there are views that have described cancer as a genetic disease, a metabolic disease, a stem cell disease, an infectious disease, a tissue disintegration disease, or a behavioral-functional disorder of cellular tissue, decoding the structural data of the images that have been done by the use of four image processing methods; Structural Density, Density Sequences (in the form of Linear-Templates and Nonlinear-Templates), Distance of Important Linear Sequences (in two ways, Linear domain difference, and Nonlinear relationship), Width Morphology (total domains and highlighted domains), showed the similarity of these phenomena with each other as well as other phenomena of the world considering different time, place and scale. Moreover, encrypted data from patterns illustrated an argument on the interaction between these phenomena. Additionally, in this article, an argument has been made that does not conflict with competing theoretical views in explaining the cause of cancer, but it considers the issue more deeply. Furthermore, by examining their geometrical microstructures, it explains that this phenomenon can occur due to feedback interactions with other phenomena, including the black hole in galaxy M87 and the aurora of the planet Saturn. In addition, according to the theory of hidden interaction, the interactive cycle of this phenomenon is expressed.

Keywords: *Interactive, Geometric, Breast-Cancer, Glioblastoma-tumors, Encrypted.*

Hossein Moradi*

Young Researchers and Elites Club, Najafabad Branch, Islamic Azad University, Najafabad, Iran.

**Email:* hosseinmoradi.ra@gmail.com

Introduction

While looking for geometric structures from recorded images of natural phenomena, I came across images with a circular appearance and concentric curves created by recording the energy emitted from phenomena at different scales and conditions. By studying the origin of these patterns, I came across the following sentences:

"… causes are still elusive and there is confusion in the literature between cause and mechanism" [1]; "The molecular basis for this response is not well understood" [2]; "while not currently well understood" [3]; "enigmatic structure" [4]; "unknown cause" [5].

Although the interactions between phenomena have been revealed in science, we are not yet aware of many interactions between phenomena to their environment and we do not have a full understanding of their communication, even in introducing them whether they are happening by chance or not. Since the study of patterns emitted from phenomena can provide valuable information about their nature and functionality, I will examine the appearance and finding patterns between the morphological data, because I believe it completely changes our view toward understanding the universe, from the behavior of the largest nebula galaxy to the evolution of diseases, fungi, and organs in nature.

This study geometrically examines three recorded images of a pattern of MCF-7 Breast Cancer Cells phenomenon (PCC) and patterns of glioblastoma tumor phenomenon (PCT). First, the formation and activity of the cancer phenomenon are expressed from the author's point of view. Then, the three recorded patterns are analyzed with six image processing methods to discover the orderliness and regularity within their structures.

Introduction

Cancer is a phenomenon that is still debated among scientists as to how it was created [6]. However, most scientists believe that the main cause of Cancer is the high metabolism and abundance of reactive oxygen species produced by mitochondria [7]. Assuming that high metabolism is expressed as the feedback of a healthy Cell from an external factor, then for a healthy Cell to become Cancerous, an external factor is required that a healthy Cell, according to its nature, comprehends the external factor and shows such feedback to this factor. The external agent cannot be without a source, so the external agent or signal from a source reaches the healthy Cell. Now, when a healthy Cell is the target of the source phenomenon, it perceives this signal and responds to it. This feedback sends the wrong message to the Cell nucleus and increases inflammation [8].

As a result, it causes chaos in normal Cells in a superficial expression. Collectively, this chaos is due to mutations in proto-oncogene genes to oncogenes (tumorigenesis) genes that (1) cause uncontrolled proliferation, (2) loss of normal Cell death (apoptosis), and (3) angiogenesis [9]. Previous studies have considered this chaos or behavioral-functional disorder of Cell tissue as "a multilevel evolutionary process" [10], "unwanted evolutionary disease" [11], or "evolutionary metabolic disease" [8]. According to this view, an increase in mitochondrial activity in a Breast Cancer Cell (Fig. 1A-a) or

an increase in glucose metabolism in a Cancerous tumor (Fig. 1A-b,c) is themselves feedback from the source mark. Therefore, the question that arises is, *whether what itself is the feedback from the perception of an external factor emitted from one or more sources can be described as an evolutionary or destructive process.*

Results

Structural Density (SD)

By specifying the exact boundary of each pattern (Fig. 1A-III) using image processing and modeling software, and placing 120 radii from the center on the patterns, Confluence of Radius and Edge (CRE) is shown (Fig. 1B shows a PCC pattern as a visual example) Patterns include a minimum of 2CRE and a maximum of 8CRE per radius. These CREs, which specify the density of confluence points per 1.120 of the patterns, show microstructural similarities if they are the same among the patterns (See Table 1 for the number of CREs in each pattern). In total, the data in Table 1 indicate that the number of 2CRE and 4CRE are repeated at 50% and 46%, respectively, and other CREs are more specific in the patterns. Of course, this general repetition can be expressed as the basic structures between a phenomenon and the specific repetition as distinct structures.

Density Sequences (DSe)

Investigation of similarities of repetitive Template components in 3-radial (9 degrees) ranges of CRE densities in two ways (Fig. 1B) Repetitive Linear-Template (Table 2) and Repetitive Nonlinear-Template (Table 3) shows that despite the lack of similarity in appearance (Figure 1A), all three patterns are composed of Linear-Template 2CRE, 2CRE, 2CRE (2.2.2) with a repetition rate of 32 to 45% of the whole templates. Furthermore, PTC-01 and PTC-02 patterns consist of a Linear-Template of 4.4.4 at a constant rate of 42%.

Conversely, in Nonlinear-Templates, the maximum repetition per pattern is different; for example, in the PCC pattern, 27% and 22% of the total identified templates are 422 and 226, respectively. In the PCT-01 pattern, templates 422 and 244 with a repetition rate of 34 are at the maximum of this pattern. The maximum repetition of other Nonlinear-Templates of the tumor pattern, PCT-02, is only Nonlinear-Template 440, with a repetition rate of 42%.

In general, the presence of common templates can be expressed as a basic similarity among the patterns. According to Tables 2 and 3, the dispersion of the linear sequences of PCT-02 and PCT-01 patterns is almost similar, but this dispersion is different in the non-linear sequences of these patterns. On the other hand, the data shows that the distribution of non-linear sequences 222 and 220 in PCT-02 and PCC patterns is similar.

Distance of Important Linear Sequences (DILS)

To understand the geometric morphological system of patterns, the position data of repetitive linear sequences are examined in two ways: A- Linear domain difference between structures (Zoning Domain), B- Nonlinear relationship of similar structures.

A- The data in Table 4, which can be used to compare the location principles of density sequences indicates the number of repetitions of the Zoning Domain differences between the positions of the linear repetitive sequences (Zoning Overlap) in each pattern (Fig. 1C shows the Zoning Overlap position in the PCC pattern as a visual example). The 514 separated Zoning Domain in Table 4 shows that the PCT-02 pattern shows the most uniform scattering, and the PCT-01 pattern shows the most non-uniform scattering of the domains created between its sequences. According to these data, the dispersion of three domains 0°-14°, 60°-74°, and 120°-134° in the PCT-01 pattern have similar ratios of 15%. This relative similarity is also observed in two other patterns, including in the PCT-02 pattern, which has a relatively constant dispersion in 9 ranges. Also, the data shows that PCC and PCT-01 patterns have almost the same dispersion in 4 domains.

B- Examining the non-linear relationship (triangular system) among the linear constant sequences shows that there are 21 sequences with the triangular system among the patterns (See Table 5 and Figure 1C in the section marked with a rectangle that shows this relationship as an example). These data show that 54° of the linear sequences of the PCT-01 pattern and 135° of the linear sequences of the PCC pattern follow this nonlinear system, and also suggest that this similarity is formed from the common linear sequence (2.2.4).

Width Morphology

The width of each pattern in 1/120 obtained using the Corresponding 1D signature technique (Fig. 2B) showed similar widths to be found among the widths data. In this regard, the study of the number of repetitions of similar widths in each pattern compared to the total width repetitions of the pattern (Table 6) shows that the maximum repetition of the width of the patterns of the Cancerous tumor phenomenon (PCT-01 and PCT-02), is at a fixed Distance (Distance19) if the width distribution of these patterns is different from each other. Table 6 also shows the narrowest and most concentrated (most minor width) pattern related to the Breast Cancer Cell phenomenon (pattern PCC). In contrast, the PCT-02 pattern of the Cancerous tumor phenomenon is The most expansive and most scattered pattern among the other patterns.

After examining the same widths in all the domains of each pattern, in order to further investigate the principles of locating the sequences; the width data of each pattern in relation to the domains of the presence of zoning overlaps are studied. Table 7 shows the similarities between patterns regarding the widths

of each pattern in Zoning Overlap as Width of Zoning Overlap (WZO) (see Tables 8, 9). The data shows that the PCC pattern in this analytical method is 45% similar to the PCT-01 pattern and 30% similar to the PCT-02 pattern. However, Cancerous tumor-related patterns are 25% similar to each other despite their presence in the same phenomenon.

Approach and Discussion

The investigation of the structures studied in this study has revealed the results of principles in complex and systematic structures. For example, the basic structures presented in the Structural Density (SD) analysis can be the origin of the structural systems of a pattern. According to this view, if two patterns are similar in terms of CRE density, the patterns use a common alphabet. For example, the similar scatter of 2CRE and 4CRE among patterns of Cancer Cell and Cancerous Tumors phenomena, especially among Cancerous Tumors patterns. The lack of CRE8 is also one of the similarities between CRE patterns PCT-02 and PCC.

On the other hand, if DILS analysis is expressed as structural locating principles, and DSe analysis (linear and nonlinear sequence repetition) is expressed as the basic similarity, then all three patterns have a basic similarity with each other considering the rate of 50% in terms of the number of repetitions of the extracted patterns; especially between two patterns PTC-01 and PTC-02, which basic similarity rate is about 84% of all linear patterns. Moreover, the similarity of the dispersion of geometric components among the PCC and PCT-01 patterns, in section A of the DILS analysis, as well as the common presence of the linear sequence 2.2.4 with the non-linear structural system in the other section of the DILS analysis, shows that the two patterns PCC and PCT-01 are composed of a common system in terms of structural placement principles. In addition to these results, the data in the WZO analysis showed that despite the difference in the type of cancer, the PCC pattern is similar to the PCT-01 pattern in 45% of the width data in Zoning Overlap, which this similarity among the registered patterns of cancer tumors (PCT-01 and PCT-02) is 25%.

Examining the recorded images of other natural phenomena in the book Hidden Interaction Theory, which were selected with different nature, behavior, and scales, including the results of more similarities of cancer patterns with other phenomena such as the black hole, Saturn's aurora borealis (12).

Comparing the Structural Density (SD), Width Morphology, Fibonacci Sequence (FS), and The Slope of Width Change Chart (SWC) analysis results showed that the Cancer Cell, Saturn, and Black hole phenomena have relative similarities. Among these similarities, the SWC analysis expresses the priority interactions between the phenomenon and the factor of the order of interactions of the Cell, Saturn, and Black hole phenomena. The Cancer Cell phenomenon is in the low priority of interaction for the Saturn and Black hole phenomena. At the same time, the structural data show the Saturn and Black hole phenomena as the main priorities of similarity between the phenomenon for the Cancer Cell phenomenon. This is while Saturn and Black holes are in the main priorities of similarity of each other. Another point of this three-phenomenon similarity is that in Width Morphology analysis, although the Cancer Cell phenomenon in the Black hole is the highest priority, the Cancer Cell phenomenon and the Blackhole are in the similarity priorities of the Saturn phenomenon, and Saturn is in similarity priority of Cancer Cell, but the Blackhole phenomenon is in low priority for the Cancer Cell. Therefore, regarding these results, *can these priority discrepancies be considered as a reason for more complex effects and being affected in a multi-phenomenon interactive cycle?* Moreover, *Can the similarities in the different analytical categories of this study and the contradiction in prioritizing these similarities be considered as interactions leading to the creation of Communication interaction cycles between phenomena?*

If we imagine a cycle of interaction as basically including influential phenomena (source phenomenon), influential factors, affected phenomena (target phenomenon), and factors representing being affected, now consider this cycle as a conference hall with its constituent people. The speaker and the audience are expressed as influential phenomena and affected phenomena. The speaker provides feedback to the audience from all or part (but under the influence of all) of the inputs of his or her mind that he or she has achieved in the past and present. This feedback becomes a factor in influencing the audience. The speaker needs a structurally shared expression with the audience to express his or her thoughts (for example, a common language). Considering all these issues, when the speaker begins to express his or her feedback of thought, the audience receives the expression in two main ways, visual and auditory, and at two levels, the concept of appearance and the concept behind appearances. Although there is no certainty in receiving the influential factor for all of the audience, if a number of the audience receive the influential factor (hear or listen to the speaker), each of these participants is considered as an affected factor and the influential factor (speech) is analyzed in regards to the nature of each person and each person creates a perception of it. These perceptions can be placed in various categories and then considered as an influential issue on the individual's perceptual system, and each person shows visible and invisible feedback to the perception of the influential factor, and this feedback indicates being affected by the influential factor. For example, the speaker says something (influential factor), and the audience

hears it and behaves toward it in the form of laughter (visible feedback), in this case, the feedback of the person is the behavior of laughing, which indicates the effectiveness of the speaker's speech. It can also be understood that if there was no speech, there would be no laughter, so there is a sign of influence when there is an influential factor. On the other hand, the other attendees' feedback may be something else. For example, one person may not show any feedback at that moment (feedback is invisible) and the other person may even be angry (feedback is visible). It should be noted that since each person has a specific nature and perceptions of the past, as a result, he expresses a different way of perceiving himself. Despite the influence of the speaker and being affected by the audience, it should be noted that this influence is not one-sided, but if the audience does not emit visible feedback, invisible feedback, although small, occurs, which informs the speaker of the effectiveness of his speech. In this case, the effect of the feedback emitted from the audience during the speech on the speaker can continue and strengthen this interaction and may even have the opposite effect. If there is continuity in the interaction, it will create an interactive cycle between them, but it may never lead to the formation of a communication interaction between the speaker and the audience. Now imagine the speaker continuing his speech, one of the attendees asks a question from the topics raised, and the speaker answers it with a little reflection, now the conference hall enters a new cycle of interaction, a cycle of the audience that has an affected position but now it is in an influential position and puts the speaker in an affected position because the question (influencing factor) reaches the speaker and the speaker reflects on his perception of the answer to the question. After that, the speaker will continue his speech by considering his affected feedback system by the influential factor (question) of the questioner. In this case, a cycle of communication interaction is created between the speaker and the questioner from the feedback generated from the past to the present of the questioner and the speaker, and this feedback is generated by each a complex interactive cycle. Now, the rest of the audience does not have only one influential factor, but also two influential ones, which makes their feedback more complex than the influential factors. At the time of the speaker's answer to the question, the conference hall includes primary influential phenomenon (speaker), primarily affected phenomena (all attendees), secondary influential phenomenon (questioner), and secondarily affected phenomena (speaker and attendees except the questioner). And in the post-response time, the conference room enters a complex cycle of interactions between influencers and affected factors. Although this complex cycle can eventually lead to chaos in identifying how interactions take place in the conference room, this chaos follows a complex system, a system in which all phenomena interact with each other, but these interactions are formed with different characteristics, just as by examining the speech of the speaker and the questioner, there are semantically common structures between their speeches, because each speech is a feedback from the opposite speech. However, it should be borne in mind that these common structures are very intense at certain intervals, and over time since the last communication interaction, the intensity of their common structures gradually decreases, and the structures that make up their feedback are formed under other interactive cycles.

Now imagine an international conference hall that does not have a fixed speaker, and anyone present of any nationality can be a speaker. Considering the phenomena as people present in the conference hall, then the universe is placed as the conference hall. Although this is a place where each person can interact or even communicate with others in their way, they need language as a common means of communication so that they can know how each other response to their words. These words are influential factors. Considering the similar results of all patterns as a basis, which was obtained from the morphological analysis of the patterns emitted from each phenomenon in this study, we can say that the people present in the conference hall used a single language, the way of communication that has been able to create basic interactions between phenomena. Another result of this study is to find structural similarities between the three phenomena of Cancer Cells, Saturn, and Black holes, similarities that vary in detail. In fact, there are similar structures between these phenomena, such as the existence of common semantic structures between the words of a speaker and a person questioning the issues raised by the speaker. Although there are semantically common structures between the words of the speaker, and the questioner, but also, there may be common superficial structures (words and letters) between their words.

In general, the existence of common structures, both semantically (invisible) and apparently (visible) between these phenomena causes chaos in the identification of influential and affected factors, but by examining the data more closely with regard to the similarities between the phenomena and considering the prioritization discrepancies in some of these similarities, it will be possible to guess the existence of influential and affected factor more concretely. For example, considering that pattern A is structurally most similar to pattern B as to other patterns, and also that the most structural similarity of pattern B is pattern C, pattern A has a low priority for pattern B. Now back to the conference hall, in this case, because the structures of a question posed from the speeches of a speaker have one part of the structures of the speeches of the speaker and also the answer to a question, have structures similar to the question and on the other hand, the question can have different structures with the answer, because the answer

is for the question, but the question is not asked for that answer (specific answer), but different answers can be given to that question. With this argument, if we consider the question and answer as influential factors or the same feedback of each phenomenon (patterns), then in the example given, pattern B (influential factor B) is a question for a phenomenon whose response (feedback) created pattern A. Additionally, pattern B is a response to pattern C because of its similar priority to pattern C. In this case, the phenomena that make up these feedbacks (patterns) interact with each other in a chain. Now, if the results show that the similarity priority of pattern C is pattern A, this chain is created as a closed chain of communication interactions of these three phenomena as an interactive cycle. When we compare this cycle with the cycle created by the feedback emitted from the audience during the lecture on the speaker, then we can deduce that the feedback generated in the interactive communication cycle can itself perpetuate and strengthen this cycle (just as by comparing this issue in everyday life in human societies, a word or behavior that itself influences other phenomena in the cycle can be a factor considering the survival of the phenomenon or vice versa). In this case, *if one of the pillars of an interactive cycle is lost for any reason or its intrinsic activity is disrupted, how will this interactive cycle continue to operate? Also, is it true that the phenomenon that is present in the inter-cosmic interaction is destroyed or an unconscious effect is placed on it?*

Although the interactions between the phenomena have not yet been inferred, the data seem to reflect the interactions between them, and despite their presence at different scales and biological natures and even their apparent dissimilarity, they indicate structures that are very similar to each other. Although the results indicate a systematic structure among all patterns, the degree of similarity and similarity of priorities indicate that they are in specific interactive cycles that prioritize interactions with each other. However, although Black holes and Cancer are among the most unknown phenomena, and the formation of Saturn is among the most complex issues in planetary science, humans do not have accurate knowledge of these phenomena; on the other hand, the comparison of the morphology of the feedback structures and the investigation of cryptography express knowledge about the lawfulness of the feedback interactions between these phenomena, although in a basic way.

In fact, common apparent structures (circular structures or concentric arcs) are not only among the phenomena of this study but there are other complex phenomena in nature (Fig. 3) that emit these structures as patterns. Including the two aurorae of the planet Earth (Fig. 3A-1) and the planet Jupiter (Fig. 3A-2), which are formed by the collision of the solar wind with the planet's magnetosphere [13-15], while Jupiter, on the other hand, gets most of the energy used to produce aurora from its rotation [16]. Other patterns formed on the surface of the planets include the two craters of Tenomer (Fig. 3B) and Richat structure (Fig. 3C) from Earth and the Poe Crater from Mercury (Fig. 3D). It is noteworthy that the formation of the Richat structure and Tenomer craters is not yet definitively clear [4], especially the Richat structure, which is still a rare, complex structure with an unknown origin [17], [18]. On the other hand, the phenomenon of Einstein's gravitational lens also creates patterns similar to the patterns in this study. Additionally, these patterns, or Einstein rings (Fig. 3E), are created by the bending of light emitted from a source or background sources as it passes by a heavy object [19] and can provide insights into dark matter, dark energy, the nature of distant universes, and even the curvature of the universe [20]. Another phenomenon with a similar structure is sarcoidosis, which with skin complications is often seen in the form of circles and wide ovals [21], [22] (Fig. 3F-1). The disease, which disrupts the normal growth of Cells (granulomas), is not a Cancer and is just a collection of inflamed Cells [23], the cause of which is still unknown [5], [24]. Also, among other skin diseases, we can mention Lupus erythematosus tumidus (LET), a form of chronic cutaneous lupus erythematosus (CLE) [25]. Figure 3F-2 shows a skin complication of a 31-year-old Caucasian female with a new, slightly pruritic rash on her upper thighs bilaterally. Other patterns created by the Blackhole include images of concentric circles centered on the CYGNI V404 Black hole (Fig. 3G), captured by Chandra and Swift. The X-ray emission energy of this Black hole is provided by an active star near the Black hole, and the researchers of this project express the empty spaces between the rings as dust in the space between us and the Blackhole [26]. In addition to the Cancerous tumor samples described in the analysis of the article, Figure 3H, also shows a PET scan of a person with liver Cancer [27]. Other patterns include images obtained from digital holographic microscopy (DHM), which are used to study the morphological features and membrane fluctuations of red blood Cells [28] (Fig. 3I). A phenomenon that its collection was an influential factor in the formation of patterns represented by the Heart. There is also evidence in other data to suggest that neurons, in order to accomplish their functional goals, regardless of their environmental noise and structural disturbances, produce intrinsic oscillations such as Figure 3J [29], oscillations that, by examining better and more closely, relative similarities of the common structure with other resulting patterns can be noted.

Conclusion

This study demonstrates the regularity and systematicity of feedback structures among world phenomena, focusing on the phenomenon of cancer, which is expressed by comparing morphology and examining their structural cryptography. A

law that showed that phenomena interact with each other in complex cycles. Cycles are expressed by four main elements: source phenomenon, influencing factor, target phenomenon, and affected factor. According to the results of this research, we found that cells are the target phenomenon or even the source phenomenon in interactive cycles with other natural phenomena. Due to the microstructural similarities and codes in each pattern, previous studies showed that part of these hidden interactions can be with the phenomenon of black holes and the planet Saturn. In this cycle, how to increase the metabolism of cancer cells, which is shown in Positron Emission Tomography (PET) imaging, is the factor that illustrates effectiveness or the influencing factor. Moreover, from another point of view, it can be said that the black hole phenomenon or even the planet Saturn can be the source phenomenon of this cycle. In this case, the cell is the target phenomenon of these sources.

Since the phenomena of the source and the target are living in different places, it must take time for the influential factor of the source to reach the target, and the question arises here is that, *whether it is possible to predict its effects by observing and examining the influencing factor emitted from the source before reaching the target phenomenon?*

And is it possible to recognize how the phenomenon is affected? or even manipulated? Because this effect is the cause of feedback, the feedback that becomes an influential factor after being emitted from the target phenomenon or even this effect causes the disappearance or causes the continuation of the life of the phenomenon.

There are other cases, too, where the semantic meaning of these structures is very valuable and can help us realize that human presence and creation have a trans-social purpose (human communities). Observations seem to show that phenomena can be studied with a holistic view and not lost in the details so that we can understand the science behind phenomena' appearances, considering that knowing a lot helps to understand the whole system of phenomena. Research on these phenomena has shown Positron Emission Tomography (PET) images, which show high metabolism in a Cancer patient, cannot be used only to diagnose the extent of preoperative injury [30], [31]; instead, the way it is metabolized, which emits magnetic charges, shows a similar pattern to other phenomena of existence, even at different times, places, and scales. It also seems that Saturn's aurorae are not just an interaction of Saturn's magnetosphere but has a function beyond the meaning we have ever had, or even a Black hole as one of the most challenging phenomena can be a transfer agent, a transfer that has only the position of classifying and synthesizing optical photons of sources, sources about which we do not yet know or have seen.

Also, many challenges and questions need more clarification before understanding the concepts of interaction between phenomena, and it is suggested that researchers and philosophers study interactions of phenomena from a different perspectives. Studies show that the use of quantum gravity theory and string theory can be a potential help in this regard. However, superficial regularities have now been discovered among the feedback structures of the phenomena and the goal seems more achievable. The discovery of hidden interactions between phenomena, recorded from the study of morphological structures of existing images, leads us to the special imaging of this research to conclude this research more comprehensively and accurately, which not only has the potential to provide a better understanding of phenomena that still hold secret information, but also to provide new insights into the field of science. I also emphasize that if an image is captured to study these structures, it can provide more accurate access to how the hidden interactive cycles, the rules in the pattern structure, and the understanding behind these rules open the door to the super humanistic sciences.

Materials and Methods

the recorded images of the Cancer phenomenon are by redox imaging of MCF-7 Breast Cancer Cells in the micropatterned tumor-stromal assay (μTSA) (Fig. 1A-a). These images have been used as a model to investigate the role of stromal constraints in altering the mitochondrial activities of Cancer Cells within the tumor microenvironment (TME). Adapted from [32]. Other images of the Cancer phenomenon are Figures 1A-b and 1A-c, which are recorded by the use of 18F-FDG (adapted from Ref. [33]) and 68Ga-DOTATOC (adapted from Ref. [34]) detectors, respectively, in positron emission tomography (PET) imaging of the most invasive type of Cancer, glioblastoma that begins in the brain [35]. These detectors have a high potential for detecting Tumors in the body by showing an increase in glucose metabolism in the vicinity of the tumor.

Image processing: For the morphology of these images, first using the Fast Fourier Transform (FFT) technique, the exact boundary of each pattern was determined (Fig. 1A-III), and the demarcated images were then converted into vectors using the Vectorize plugin in Rhinoceros software; finally, a hypothetical circle was created on the patterns by HoughCircles circle detection using OpenCV and python. Subsequently, to obtain the morphological information of the components of each pattern, 120 radiuses were passed from the center of this circle (the distance between each radius is 3 degrees). For example, the PCC pattern of the Saturn phenomenon is shown along with the radial lines drawn in Figure 1B.

Structural density investigation: To determine the density of the boundaries taken from the patterns, the intersection points

of the 3-degree radii with the boundaries taken in AutoCAD software were investigated. In this case, odd CREs are created, which were not considered due to the frequency of less than 2% of this data, and the intersection data with the even categories of CREs are presented in Table 1.

Radial ranges (Density Sequences): To evaluate the pattern components in more common domains, 3-radius (9-degree) ranges of CRE densities were considered as density sequences. Density sequences were investigated in two ways: (1) 3 radial sequences with linear connection (Linear-Template) which is created by examining 3 radiuses as chains next to each other, and (2) 3 radial sequences with nonlinear-template connection, which is created by connecting radii with an angle difference of 120 degrees to each other. These two methods are visually demonstrated in Figure 1B. In total, each pattern consists of 118 linear sequences and 120 nonlinear sequences, which are created by considering 3 patterns, 354 linear sequences, and 360 nonlinear sequences. Due to a large number of sequences in the number of common repetitions between patterns, sequences with more than 10 repetitions were presented as linear repetitive sequences in Table 2 and nonlinear repetitive sequences in Table 3.

Distance of Important Linear Sequences (DILS): To investigate the location order of density sequences, the position of linearly repeated sequences in each pattern was determined and compared with each other. Since a large amount of the radii passed through the patterns included frequent sequences 2.2.2 and 4.4.4, they were ignored and the position of other frequent sequences was investigated. Finally, the locations of the presence of repetitive linear sequences in the patterns were introduced as Zoning Overlap (Fig. 1C shows the location of Zoning Overlap in the PCC pattern). The distance between the Zoning Overlaps, called the Zoning Domain, was divided into 12 categories of 15 degrees. The number of Zoning Domains iterates per pattern relative to the total number of Zoning Domains available in 15-degree categories is presented in Table 4. In order to check whether linear sequences can express more complex principles in patterns or whether non-linear sequences obtained from morphology can provide regularity in a wider range of patterns, an analytical method of investigating the nonlinear relationship among linear constant sequences was performed.

This method compares and examines linear fixed sequences (9 degrees) at 120 ° intervals at 30 ° tolerance with the coordinates of nonlinear repetitive sequences (Table 10 provides a comprehensive comparison of the coordinates of each 27-degree structure with the coordinates of the nonlinear sequence). Moreover, as a visual example in the section marked with a rectangle in figure 1C; the linear sequence 2.2.4, which exists in coordinates (14.15.16), is also present in two categories of coordinates (140.141.142) and (248.249.250) which their position shows a nonlinear relationship of approximately 120 degrees. To put it simply, this method examines a 27-degree domain with fixed CRE densities in three groups of 3 radiuses of a pattern arranged in a nonlinear system. The number of iterations of these structures with the expression of the iterative sequence is presented in Table 5.

Width Morphology: To obtain the width of each pattern, two steps were performed, which are presented separately in Figure 2. First, the radius created along the confluence points of the patterns was created as a Corresponding 1D signature (Fig. 2B) and the coordinates of the CREs were determined by separating the two distance vectors from the center and the domain. Then the maximum distance between the confluence points in each domain (radius) of each pattern is calculated and expressed as the width of the pattern in that range (Figure 2C shows how to identify the width of the part of the PCC pattern as a visual example). Since each pattern has different widths, the ratio of the repetitions of the widths in each pattern to the total repetition of the widths of each pattern is calculated and shown separately in Table 6.

On the other hand, the data on the thickness of the patterns were studied with respect to the Zoning Overlaps that were stated in the investigation of the principles of the placement of the sequences. Thus, all these were done to check once again the structural system in the domains of repetitive sequences. The width of the Zoning Overlap areas of each pattern was examined and then to compare the data of these tables with each other, the prepared data from each pattern were calculated in relation to their maximum width and were in the range of 0.1 to 1. Table 8 shows the ratio of the presence of these widths to the total widths obtained in the slopes of the repetitive sequences of each pattern. Finally, these data were broken down into 5% ratios to better represent the replication of the similarity of the widths of each pattern in the overlapping regions (see Table 9). Table 9, for example, shows that the PCT-01 and PCC patterns are 15% of their thickness in the 0.5 range. This data was presented as an abstract and summary in Table 7.

Acknowledgments

I am thankful to Masoud Shams as my research assistant for analyzing the data and influencing the definition of my research direction. I'd like to express my heartfelt gratitude to Elias Aghili Dehnavi and his team for the translation technical editing.

Financial support and sponsorship

Nil.

Conflicts of interest

There are no conflicts of interest.

Data and materials availability

All data are available in the main text or the supplementary materials.

References

[1] P. Vineis, P. Illari, and F. Russo, “Causality in Cancer research: a journey through models in molecular epidemiology and their philosophical interpretation,” Emerg. Themes Epidemiol., vol. 14, no. 1, pp. 1–8, 2017, doi: 10.1186/s12982-017-0061-7.

[2] Z. Liao, D. Lockhead, E. D. Larson, and C. Proenza, “Phosphorylation and modulation of hyperpolarization-activated HCN4 channels by protein kinase A in the mouse sinoatrial node,” J. Gen. Physiol., vol. 136, no. 3, pp. 247–258, 2010, doi: 10.1085/jgp.201010488.

[3] B. H. Mauk, J. T. Clarke, D. Grodent, J. H. Waite, C. P. Paranicas, and D. J. Williams, “Transient aurora on Jupiter from injections of magnetospheric electrons,” Nature, vol. 415, no. 6875, pp. 1003–1005, 2002, doi: 10.1038/4151003a.

[4] W. U. Reimold and C. Koeberl, “Impact structures in Africa: A review,” J. African Earth Sci., vol. 93, no. January, pp. 57–175, 2014, doi: 10.1016/j.jafrearsci.2014.01.008.

[5] S. Lodha, M. Sanchez, and S. Prystowsky, “Recent Advances in Chest Medicine Sarcoidosis of the Skin A Review for the Pulmonologist,” Chest, vol. 136, no. 2, pp. 583–596, 2009, doi: 10.1378/chest.08-1527.

[6] A. Plutynski, “Is Cancer a matter of luck?” Biol. Philos., vol. 36, no. 1, pp. 1–28, 2021, doi: 10.1007/s10539-020-09778-8.

[7] P. Person, “Otto Warburg: ‘on the origin of Cancer Cells,’” Oral Surgery, Oral Med. Oral Pathol., vol. 10, no. 4, pp. 412–421, 1957, doi: 10.1016/0030-4220(57)90167-6.

[8] S. Zaminpira and S. Niknamian, “How Butterfly Effect or Deterministic Chaos Theory in Theoretical Physics Explains the Main Cause of Cancer,” EC Cancer, vol. 2, no. 5, pp. 227–238, 2017.

[9] A. Plutynski, “Cancer Modeling: the Advantages and Limitations of Multiple Perspectives,” 2018.

[10] C. Lean and A. Plutynski, “The evolution of failure: explaining Cancer as an evolutionary process,” Biol. Philos., vol. 31, no. 1, pp. 39–57, 2016, doi: 10.1007/s10539-015-9511-1.

[11] I. Bozic and C. J. Wu, “from theory to reality,” Nat. Cancer, vol. 1, no. June, 2020, doi: 10.1038/s43018-020-0079-6.

[12] H. Moradi, “Hidden Interaction Theory,” tradition, 2022.

[13] K. Hosokawa et al., “Multiple time-scale beats in aurora: precise orchestration via magnetospheric chorus waves,” Sci. Rep., vol. 10, no. 1, p. 3380, 2020, doi: 10.1038/s41598-020-59642-8.

[14] J. T. Clarke et al., “Ultraviolet emissions from the magnetic footprints of Io, Ganymede and Europa on Jupiter,” Nature, vol. 415, no. 6875, pp. 997–1000, 2002, doi: 10.1038/415997a.

[15] S. W. H. Cowley and E. J. Bunce, “Origin of the main auroral oval in Jupiter’s coupled magnetosphere-ionosphere system,” Planet. Space Sci., vol. 49, no. 10–11, pp. 1067–1088, 2001, doi: 10.1016/S0032-0633(00)00167-7.

[16] J. Saur, E. Chané, and O. Hartkorn, “Modeling Magnetospheric Fields in the Jupiter System,” pp. 153–182, 2018, doi: 10.1007/978-3-319-64292-5_6.

[17] R. S. DIETZ, “Roter Kamm, Southwest Africa: Probable Meteorite Crater,” Meteoritics, vol. 2, no. 4, pp. 311–314, 1965, doi: https://doi.org/10.1111/j.1945-5100.1965.tb01438.x.

[18] J. H. Freeberg, Terrestrial Impact Structures: A Bibliography, 1965-68. U.S. Government Printing Office, 1969.

[19] T. E. Collett et al., “A precise extragalactic test of general relativity,” Science (80-.)., vol. 360, no. 6395, pp. 1342–1346, 2018, doi: 10.1126/science.aao2469.

[20] NASA, ESA, R. Gavazzi, T. Treu, and SLACS team, “Hubble Finds Double Einstein Ring.” 2008, [Online]. Available: http://hubblesite.org/newscenter/archive/releases/2008/04/image/a/.

[21] J. Mu et al., “Genetics of Sarcoidosis,” vol. 29, pp. 391–414, 2008, doi: 10.1016/j.ccm.2008.03.007.

[22] S. Imadojemu, M. B. E. Karol, M. Noe, M. Joseph, C. E. Iii, and M. Rosenbach, “Cutaneous Sarcoidosis,” 2019, doi: 10.1016/B978-0-323-54429-0.00011-2.

[23] A. Haimovic, M. Sanchez, M. A. Judson, and S. Prystowsky, “Sarcoidosis : A comprehensive review and update for the dermatologist,” J. Am. Dermatology, vol. 66, no. 5, pp. 719.e1-719.e10, doi: 10.1016/j.jaad.2012.02.003.

[24] I. Chikeka, S. Husain, and M. E. Grossman, “Asymptomatic annular perianal sarcoidosis,” JAAD Case Reports, vol. 6, no. 12, pp. 1242–1244, 2020, doi: 10.1016/j.jdcr.2020.09.009.

[25] J. Stead, C. Headley, M. Ioffreda, C. Kovarik, and V. Werth, “Coexistence of Tumid Lupus Erythematosus with Systemic Lupus Erythematosus and Discoid Lupus Erythematosus: A Report of 2 cases,” vol. 14, no. 6, pp. 338–341, 2010, doi: 10.1097/RHU.0b013e31817d1183.Coexistence.

[26] S. Heinz et al., “ a Joint Chandra and Swift View of the 2015 X-Ray Dust-Scattering Echo of V404 Cygni,” Astrophys. J., vol. 825, no. 1, p. 15, 2016, doi: 10.3847/0004-637x/825/1/15.

[27] “Secondary liver Cancer, CT and PET scans - Stock Image - C016_6770 - Science Photo Library.”, [Online]. Available: https://www.sciencephoto.com/media/520498/view/secondary-liver-cancer-ct-and-pet-scans

[28] K. W. Seo, E. Seo, and S. J. Lee, “Cellular imaging using phase holographic microscopy: For the study of the pathophysiology of red blood cells and human umbilical vein endothelial Cells,” J. Vis., vol. 17, no. 3, pp. 235–244, 2014, doi: 10.1007/s12650-014-0200-y.

[29] M. I. Rabinovich, P. Varona, and H. D. I. Abarbanel, “Nonlinear cooperative dynamics of living neurons,” Int. J. Bifurcation. Chaos, vol. 10, no. 5, pp. 913–933, 2000, doi: 10.1142/S0218127400000669.

[30] G. Sgouros et al., “Patient-specific dosimetry for 131I thyroid Cancer therapy using 124I PET and 3-Dimensional-Internal Dosimetry (3D-ID) software,” J. Nucl. Med., vol. 45, no. 8, pp. 1366–1372, 2004.

[31] D. Wu, D. Ylli, S. L. Heimlich, K. D. Burman, L. Wartofsky, and D. Van Nostrand, “(124)I Positron Emission Tomography/Computed Tomography Versus Conventional Radioiodine Imaging in Differentiated Thyroid Cancer: A Review.,” Thyroid, vol. 29, no. 11, pp. 1523–1535, Nov. 2019, doi: 10.1089/thy.2018.0598.

[32] H. M. Begum et al., “Spatial Regulation of Mitochondrial Heterogeneity by Stromal Confinement in Micropatterned Tumor Models,” Sci. Rep., vol. 9, no. 1, p. 11187, 2019, doi: 10.1038/s41598-019-47593-8.

[33] J. BOLCAEN et al., “PET for Therapy Response Assessment in Glioblastoma,” Glioblastoma, pp. 175–195, 2017, doi: 10.15586/codon.glioblastoma.2017.ch10.

[34] D. Heute et al., “Response of recurrent high-grade glioma to treatment with 90Y-DOTATOC,” J. Nucl. Med., vol. 51, no. 3, pp. 397–400, 2010, doi: 10.2967/jnumed.109.072819.

[35] F. E. Bleeker, R. J. Molenaar, and S. Leenstra, “Recent advances in the molecular understanding of glioblastoma,” J. Neurooncol., vol. 108, no. 1, pp. 11–27, 2012, doi: 10.1007/s11060-011-0793-0.

[36] “IMAGE Spacecraft Pictures Aurora.” 2006, [Online]. Available: https://earthobservatory.nasa.gov/images/6226/image-spacecraft-pictures-aurora.

[37] “An unexpected source of energy for the auroras of Jupiter.”, [Online]. Available: https://www.news.uliege.be/cms/c_9314641/en/an-unexpected-source-of-energy-for-the-auroras-of-jupiter.

[38] “Tennoumer topographic map, elevation, relief.”, [Online]. Available: https://en-nz.topographic-map.com/maps/os0y/Tennoumer/.

[39] "Richat Structure." 2014, [Online]. Available: https://en.wikipedia.org/w/index.php?title=Richat_Structure&oldid=603695071.

[40] "Richat Structure topographic map, elevation, relief.", [Online]. Available: https://en-us.topographic-map.com/maps/9ynj/Richat-Structure/.

[41] G. Matton and M. Jébrak, "The 'eye of Africa' (Richat dome, Mauritania): An isolated Cretaceous alkaline-hydrothermal complex," J. African Earth Sci., vol. 97, pp. 109–124, 2014, doi: 10.1016/j.jafrearsci.2014.04.006.

Figures and Tables

[42] NASA/JPL, "Catalog Page for PIA05580." 2004, [Online]. Available: https://photojournal.jpl.nasa.gov/catalog/PIA02653%0Ahttps://photojournal.jpl.nasa.gov/catalog/PIA05580.

[43] "Dermatologic Manifestations of Sarcoidosis: Overview, Physical Examination, Differential Diagnosis." [Online]. Available: https://emedicine.medscape.com/article/1123970-overview#a2.

[44] "Chandra __ Photo Album __ V404 Cygni __ August 5, 2021.", [Online]. Available: https://chandra.harvard.edu/photo/2021/v404cyg/.

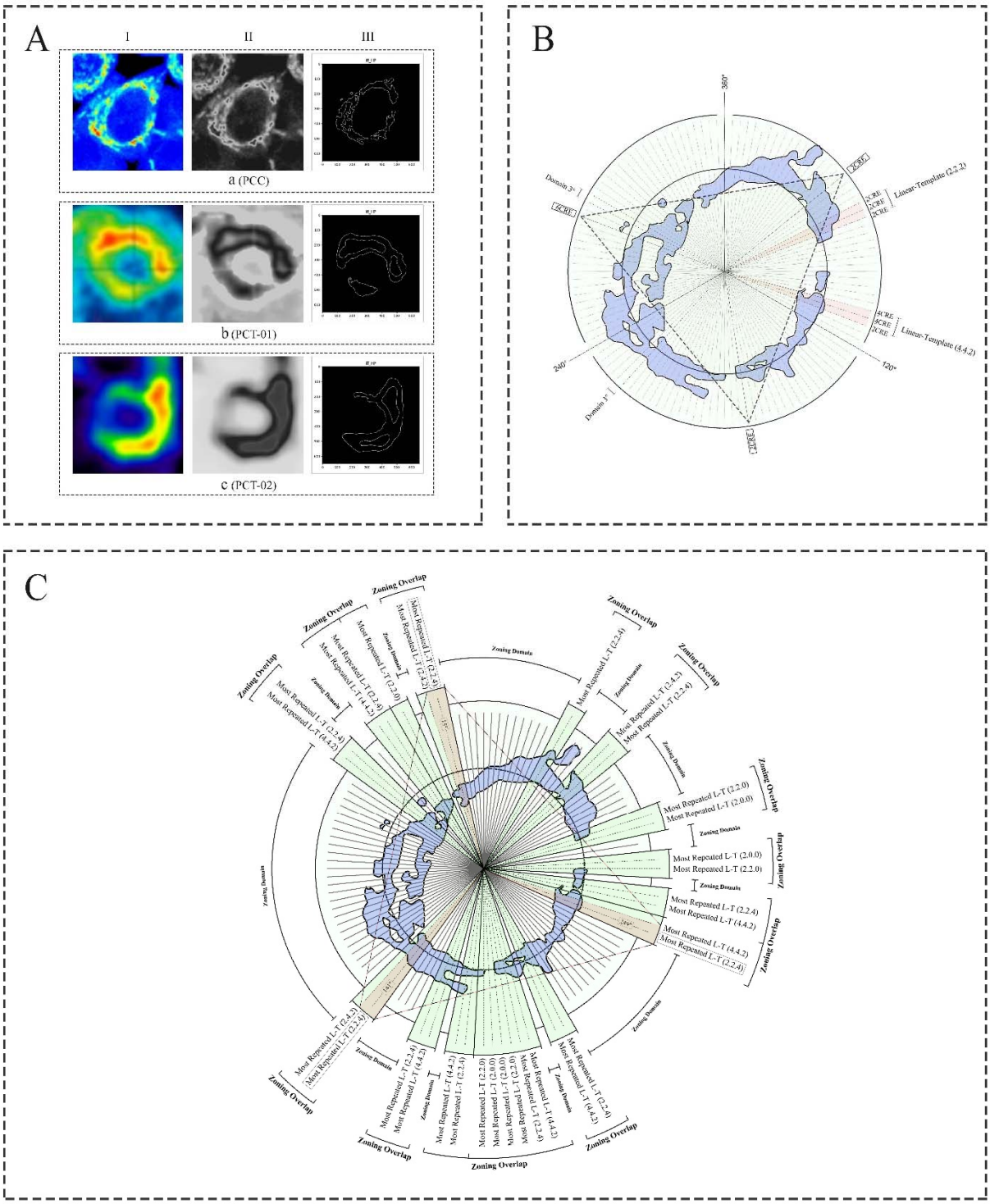

Fig. 1. (A) Case studies. (I) images of the recorded pattern from the Cancer phenomenon, **(a)** with redox imaging of MCF-7 Breast Cancer Cells (Adapted from [52]), and positron emission tomography (PET) imaging of glioblastoma by the use of **(b)** 18F-FDG (adapted from Ref. [53]) and **(c)** 68Ga-DOTATOC (adapted from Ref. [54]) detectors. **(II)** Noise-free images (preparation for fast Fourier transform). **(III)** Marginalized images by the Fourier transform technique. **(B) Confluence of Radius and Edge (CRE); creates identifiers for each radius of the pattern.** Examining these identifiers as three-radial chains next to each other forms linear sequences. Connecting these identifiers that are placed 120 degrees apart from each other, constitute nonlinear sequences. For example, three radii are connected by a dashed line, which inserting their identifiers creates the nonlinear sequence 2CRE.6CRE.2CRE. We will briefly describe it in 2.6.2. The pattern used in this image has been selected as a sample from the 14 patterns studied, which belong to the PCC pattern. **(C) The distance between key linear sequences.** Positioning the presence of repetitive linear sequences, shown as Zoning Overlap, identifies parts of the pattern that, by examining the distance between them as the Zoning Domain, can provide the principles for locating the density sequences of each pattern. It is noteworthy that the triangular section, shown with a dashed line, illustrates a nonlinear system in repeating fixed CREs in 3 groups of 3 radial patterns. Repeatable CRE marked with a rectangle. The pattern used in this image has been selected from one of the 14 case studies and belongs to the PCC pattern.

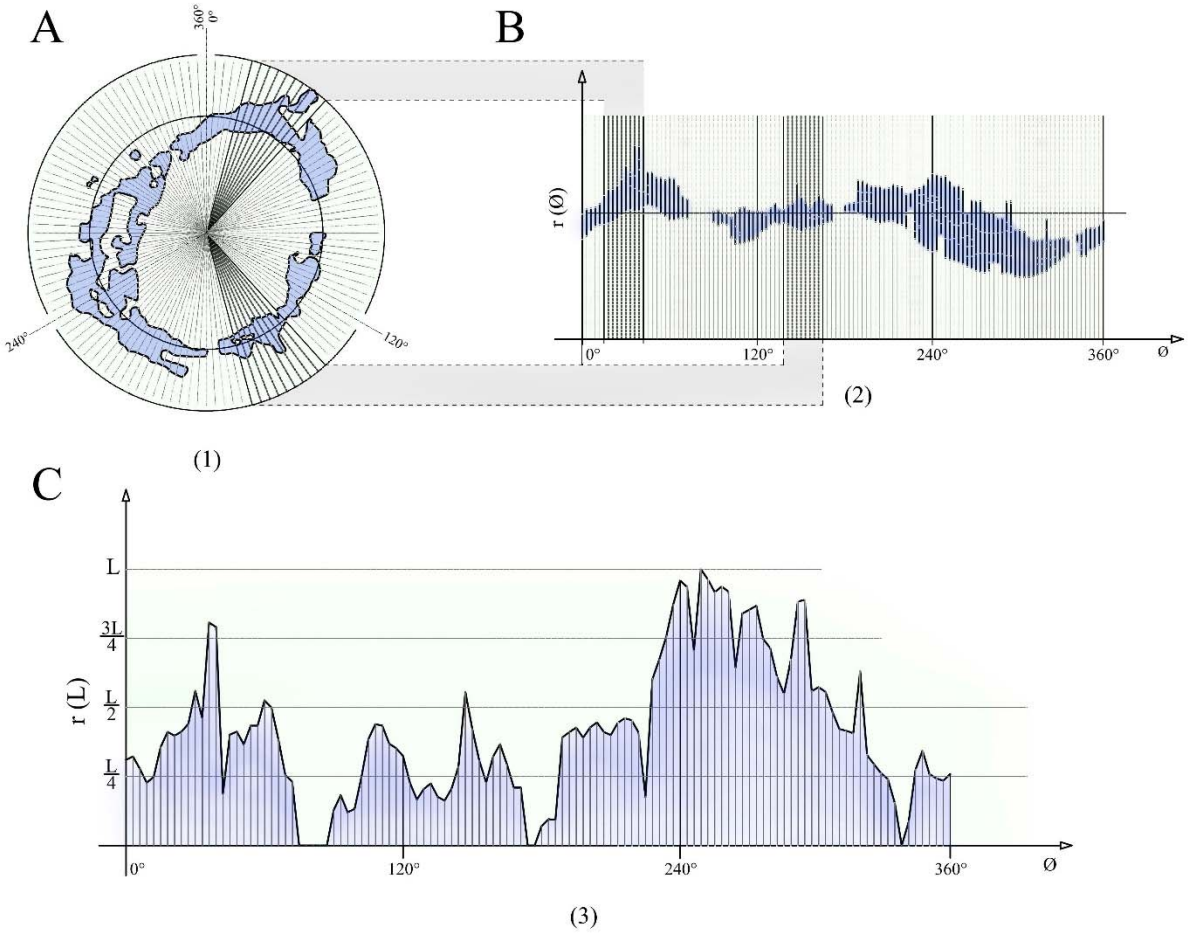

Figure 2. The changes in the pattern's thickness. (A) Pattern with 120 radius separation **(B)** Chart created by the corresponding 1D signature of radii with intersection points of the pattern on the two axes of distance from the center and the amplitude. **(C)** Graph of changes in the maximum thickness of the pattern in the 3-degree amplitude of the pattern. The magnified section shows the maximum distance between the intersection points of the pattern and the radius. The pattern used in this image has opted from the 14 case studies, which belongs to the PCC pattern.

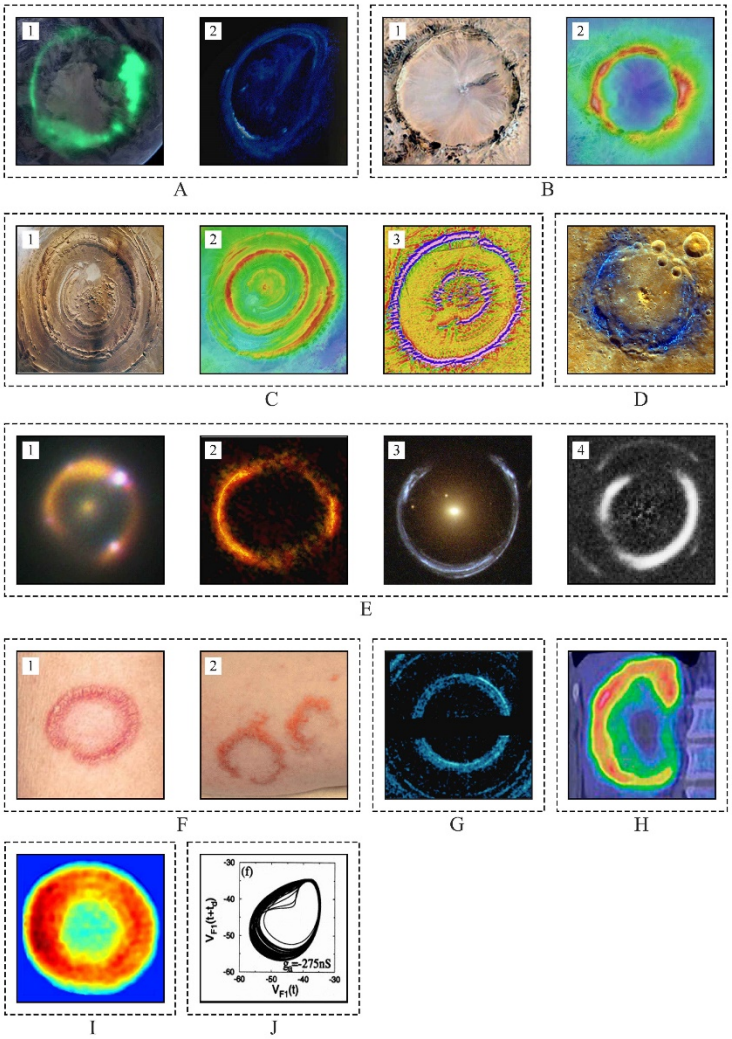

Figure 3. Other phenomena with circular structures and concentric arches in nature. (A) Two images in **(A-1)** related to the aurora phenomenon [36] and **(A-2)** related to Jupiter aurora [37]. **(B)** Tenomer crater located in the Western Sahara of Mauretania of planet earth. **(B-1)** shows the satellite image of the Tenomer crater [4], and **(B-2)** shows the topographic image of this crater [38]. **(C)** The Richat Structure, known as Guelb er Richât located in western-central Mauritania, Northwest Africa. **(C-1)** shows a satellite image [39], **(C-2)** a topographic image [40], and **(C-3**) a Magnetic survey of the Richat structure [41]. **(D)** Poe's estuary is located in the northwestern part of the Caloris Basin [42], which is a high-resolution color image. **(E)** The rings created from the alignment of the foreground and background galaxies, known as the Einstein ring, were recorded by NASA's ESA / Hubble Space Telescope. **(E-1)** The iPTF16geu supernova exploded about 4.3 billion years ago when it was illuminated by a galaxy in the foreground, making it 52 times brighter for observers on Earth. **(E-2)** Atacama Large Millimeter/submillimeter Array (ALMA) observation of the gravitationally lensed galaxy SDP.81 (its formal name is HATLAS J090311.6+003906). **(E-3)** Cosmic Horseshoe Observation Image (also known as SDSS J1148 + 1930) through the gravity field of the foreground rare galaxy, LRG 3-757. **(E-4)** Image of an unusual gravitational lens system SDSSJ0946 + 1006 with two concentric ring-like structures formed after subtracting the glare of the central, foreground galaxy. **(F)** Skin conditions commonly found on the extremities or trunk of the human body. **(F-1)** Annular appearance of sarcoidosis. Adapted from [43]. **(F-2)** Lupus erythematosus tumidus (LET) with Annular dermal plaques on the thigh. Adapted from [25]. **(G)** Features a set of rings around a Black hole, captured using NASA's Chandra X-ray Observatory and Neil Gehrels Swift Observatory. Adapted from [44]. **(H)** Secondary liver Cancer. This image is a combination of Coloured computed tomography (CT) scan and a positron emission tomography (PET) scan. Adapted from [27]. **(I)** Represents a topographic image of a typical RBC separated from the background. Adapted from [28]. **(J)** Phase portrait of the slow components of oscillations in a PD neuron as a function of the external conductance without injecting any external DC. Adapted from [29].

Table 1. The number of CREs in each pattern.

Pattern	2CRE	4CRE	6CRE	8CRE	10CRE	12CRE
PCC	67	33	11	0	0	0
	60%	30%	10%	0%	0%	0%
PCT-01	41	54	1	1	0	0
	42%	56%	1%	1%	0%	0%
PCT-02	41	46	5	0	0	0
	45%	50%	5%	0%	0%	0%

Table 2. Repetitive linear sequences. The number of 3-radial sequences with linear-template relation of CRE densities as chains next to each other. Note that these sequences are just repetitive linear sequences among patterns.

	2-2-2	4-4-4	2-4-2	4-4-2	6-4-4	4-6-6	2-4-2	6-6-6	4-6-4	2-4-6	2-2-6	4-2-4	2-6-4	0-2-2	6-6-8	6-4-6	2-0-0
PCC	52	99	11	9	9	1	1	1	1			1		1			4
	45%	88%	9%	8%	8%	0%	1%	1%	1%			1%		0%			1%
PCT-01	29	39	0	1	1	0	0	0	0	0	0	0	0	1	0	0	0
	32%	43%	0%	0%	1%	0%	0%	0%	0%	0%	0%	0%	0%	1%	0%	0%	0%
PCT-02	32	37	0	0	0	0	0	0	1	0	1	0	1	1	0	0	0
	36%	42%	0%	0%	0%	0%	0%	0%	1%	0%	1%	0%	1%	0%	0%	0%	0%

Table 3. Repetitive non-linear sequences. The number of 3-radial sequences with the nonlinear-template relationship of CRE densities with 120-degree angle difference to each other. Note that these sequences are just non-linear repetitive sequences in patterns.

	4 22	2 44	2 22	4 20	2 26	4 40	4 62	6 46	4 44	2 82	2 20
PCC	30	12	18	6	24	3	0	0	9	0	9
	27 %	11 %	16 %	5%	22 %	3%	0 %	0 %	8%	0 %	8 %
PCT-01	30	30	3	12	0	0	3	0	9	0	0
	34 %	34 %	3%	14 %	0%	0%	3 %	0 %	10 %	0 %	0 %
PCT-02	15	0	18	21	3	45	0	0	0	0	6
	14 %	0%	17 %	19 %	3%	42 %	0 %	0 %	0%	0 %	6 %

Table 4. Principles of locating repetitive linear sequences relative to each other. The 800 domains separated in this table show the Zoning Domain repetition ratio between the positions of repetitive linear sequences, or Zoning Overlap, in 12 sets of 15 degrees per pattern.

Pattern	**0°-14°**	**15°-29°**	**30°-44°**	**45°-59°**	**60°-74°**	**75°-89°**	**90°-104°**	**105°-119°**	**120°-134°**	**135°-149°**	**150°-164°**	**165°-179°**
PCC	15%	6%	6%	3%	12%	6%	-	15%	12%	3%	3%	21%
PCT-01	15%	-	-	-	15%	5%	20%	10%	15%	-	10%	10%
PCT-02	8%	11%	8%	8%	8%	9%	8%	6%	10%	9%	9%	7%

Table 5. Investigation of nonlinear relationship (triangular system) between fixed linear sequences. The table illustrates the number of repetitions in 3 fixed sets of CRE densities in 3 different radii of a pattern in a nonlinear system (in the range of 120° with a tolerance of 30°) relative to each other.

Pattern	**Nonlinear relation between Linear Templates**			**Linear Template presence**
	Count		**Linear Template**	
PCT-01	2	2	2.2.4	54 °
PCC	5	5	2.2.4	135 °

Table 6. The ratio of the repetitions of the existing thicknesses in each pattern to the total repetition, of the thicknesses of each pattern in the same units. For this unit uniformity, the patterns were changed and examined at a constant scale.

Distances	P CC	P CT-01	P CT-02
1	1%	2%	-
2	5%	2%	-
3	6%	3%	2%
4	10%	1%	4%
5	11%	1%	4%
6	6%	1%	2%
7	11%	1%	3%
8	18%	4%	2%
9	4%	6%	2%
10	5%	3%	1%
11	3%	4%	1%
12	2%	3%	1%
13	4%	2%	1%
14	2%	7%	1%
15	2%	5%	-
16	4%	5%	1%
17	4%	3%	4%
18	2%	8%	11%
19	1%	14%	20%
20	-	6%	15%
21	-	5%	7%
22	-	2%	3%
23	-	-	1%
24	-	2%	-
25	-	1%	1%
26	-	2%	-
27	-	5%	1%
28	-	1%	-
29	-	-	2%
30	-	-	-
31	-	-	1%
32	-	-	-
33	-	-	3%
34	-	-	2%
35	-	-	1%
36	-	-	-

Table 7. The similarity ratio of the thicknesses in each pattern in the Zoning Overlap among other patterns.

	PCC	PCT-01	PCT-02
PCC	-	45%	30%
PCT-01	45%	-	25%
PCT-02	30%	25%	-

Table 8. Dispersion value. The ratio of the presence of the width of the Zoning Overlap to the total widths obtained of each pattern is in the range of 0.1 to 1. these ranges are the ratio of each width to the largest width of each pattern.

Range	PCT-01	PCT-02	PCC
0.1	15%	7%	2%
0.2	15%	15%	12%
0.3	8%	7%	8%
0.4	4%		12%
0.5	12%	37%	12%
0.6	4%	15%	8%
0.7	4%		23%
0.8	19%	4%	21%
0.9	15%	4%	2%
1	4%	11%	2%

Table 9. The similarity of ranges. The presence of different widths ranges according to their dispersion value, which expresses the data in Table 7 in another way.

Dispersion value	PCT-01	PCT-02	PCC
5%		0.8	
5%		0.9	0.9
5%	1		1
5%			0.1
5%			
5%	0.6		
5%	0.4		
5%			
10%		0.1	
10%			
10%	0.3	0.3	0.3
10%			
10%			0.6
10%			
10%			
10%			
10%			
15%	0.2	0.2	0.2
15%			
15%			0.4
15%	0.5		0.5
15%		0.6	
15%			
15%			
15%	0.9		
15%		1	
20%			
25%			
25%			0.7
25%			
25%			0.8
35%			
40%			

Table 10. The nonlinear relationship between linearly fixed sequences. A comprehensive comparison of the coordinates of each 27-degree structure (of repeated Linear templates) with the coordinates of the nonlinear sequence.

		Repeated Linear templates coordinates			Repeated Non-Linear templates coordinates		
	Templates	**A**	**B**	**C**	**A**	**B**	**C**
PCT-01	**2.2.4**	72	141	312	75	195	315
	2.2.4	126	249	312			
	2.2.4	129	249	312			
	2.2.4	72	141	249	21	141	261
	4.4.2	69	132	252			
	4.4.2	132	252	315			
	4.4.2	69	138	252			
PCT-02	**2.2.4**	3	123	234			
	2.2.4	9	123	234			
	2.2.6	159	261	333			
	2.6.4	162	264	330			
	2.2.4	51	174	330			
PCC	**2.2.4**	51	192	261	51	171	291
	2.2.4	51	192	312			
	2.2.4	51	192	330			
	2.2.4	51	207	312	51	171	291
	2.2.4	51	207	330			
	2.2.4	15	141	249	15	135	255
	2.2.4	15	141	207			
	2.2.4	51	174	261			
	2.2.4	51	174	312	51	171	291
	2.2.4	15	141	261	15	135	255
	2.2.4	15	159	249			
	2.2.4	15	141	312			
	4.4.2	48	162	252			